Polymer Degradation and Stability 195 (2022) 109783

Contents lists available at ScienceDirect

Polymer Degradation and Stability

journal homepage: www.elsevier.com/locate/polymdegradstab

Investigating thermomechanical recycling of poly(ethylene terephthalate) containing phosphorus flame retardants

Christopher Bascucci[a], Ivica Duretek[b], Sandro Lehner[a], Clemens Holzer[b], Sabyasachi Gaan[a], Rudolf Hufenus[a], Ali Gooneie[a,*]

[a] Laboratory of Advanced Fibers, Empa, Swiss Federal Laboratories for Materials Science and Technology, Lerchenfeldstrasse 5, St. Gallen CH-9014, Switzerland
[b] Polymer Processing, Montanuniversitaet Leoben, Otto Gloeckel-Strasse 2, Leoben 8700, Austria

ARTICLE INFO

Article history:
Received 3 September 2021
Revised 11 November 2021
Accepted 12 November 2021
Available online 15 November 2021

Keywords:
Poly(ethylene terephthalate)
Phosphorus flame retardants
Thermomechanical recycling
Degradation and stability
Rheology

ABSTRACT

Poly(ethylene terephthalate) (PET) has wide usage in packaging and fiber industries thanks to its superior mechanical, thermal, and barrier properties. It is also one of the "big five" recyclable plastics with well-established procedures. In many textile and film products, flame retardants (FRs) are added to PET for fire-safe applications. However, PET/FR products are often not designed *for* recycling, and downgrade during thermomechanical recycling due to polymer degradation. To address this issue, we study the behavior of PET containing phosphorus FRs during and after thermomechanical recycling. Two phosphorus FRs, namely DOPO-PEPA (DP) and Aflammit PCO 900 (AF), are added to PET by extrusion. The compounds are then studied by a comprehensive set of thermal, rheological, and chemical experiments to investigate their thermal, thermo-oxidative, and thermo-mechanical degradation mechanisms. The results indicate the high potential of DP to add enhanced lubrication, and control melt rheology over long periods by stabilization. On the other hand, AF can boost chain extensions and branching in PET, which can counter chain scissions to some extent. A chemical mechanism is proposed suggesting that both FRs can release active radicals and moieties that either quench other radicals such as oxygen radicals, or initiate a reaction with the PET chains leading to chain scissions and/or branching. Finally, a thermomechanical recycling process is simulated by reprocessing the PET compounds in extrusion and injection molding. The mechanical performance of the compounds before and after recycling is studied in tensile experiments. PET/DP samples preserve their ductile tensile behavior after recycling, whereas PET/AF samples become completely brittle. This work motivates future research on the synthesis of new phosphorus FRs based on mixed chemical characteristics of DP and AF for improved recyclability of PET/FR products.

1. Introduction

Poly(ethylene terephthalate) (PET) is widely used in packaging and textiles due to its good mechanical properties, low permeability to moisture and gas, and high heat resistance [1–3]. PET yarn is used in a variety of applications including interior textiles, upholstery, and carpets in transportation [4]. In such products, it is often mandatory to add flame retardant (FR) functionality to PET to extend the time-of-escape from fire [5–8]. While the recyclability of virgin PET is well-established to be one of its main advantages, the recyclability of PET/FR products is not well addressed [2,5,9]. Due to the requirements of the circular economy, PET/FR waste must be recycled and new products must ideally be Designed *for* Recycling [9–17]. However, FR-containing plastic waste is often landfilled or recycled for energy rather than new products [5,18,19]. Moreover, the recycled plastic waste is typically upcycled by adding FR additives as a route to Design *from* Recycling [5,20]. In general, two main alternatives are adopted to recycle PET, i.e. thermomechanical and chemical recycling [2,9,21]. In the former approach, waste PET is washed and reprocessed to produce recycled flakes or pellets. On the other hand, the chemical recycling approach consists of a partial (or total) depolymerization of the material to obtain regenerated oligomers/monomers that are then re-used in a new polymerization process [1,22–24]. The chemical approach is compromised by the low yields of the reactions and produces additional solvent waste [2,9]. For this reason, thermomechanical recycling today stands as the undisputed primary recycling method of PET in Europe [25]. Thus, it is highly desirable to design FR-containing PET products that can contribute to a circular economy through thermomechanical recycling.

* Corresponding author.
E-mail address: ali.gooneie@empa.ch (A. Gooneie).

https://doi.org/10.1016/j.polymdegradstab.2021.109783

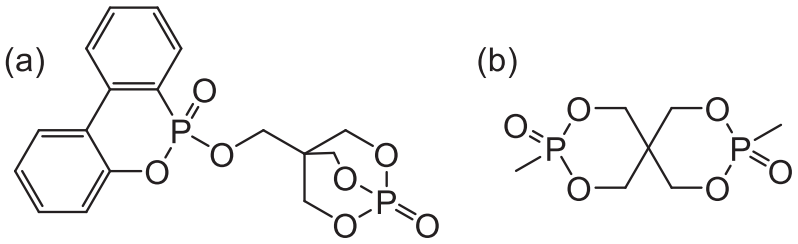

Fig. 1. Chemical structures of (a) DP, and (b) AF.

It is well-known that PET undergoes severe degradation in thermomechanical recycling, which leads to a loss of its properties, more specifically its mechanical performance [2,9,26,27]. In previous studies, we have found that phosphorus FRs, such as DOPO-PEPA (DP) and Aflammit PCO 900 (AF) (Fig. 1), have the potential to act as multifunctional additives in polyesters; they add FR properties and can control the degradation reactions during PET recycling [27–29]. Consequently, Design *for* Recycling of PET/FR products can be envisioned by means of eco-friendly phosphorus FRs. Here, we investigate the potential of such phosphorus FRs in designing PET/FR products for recycling, which is a major step toward realizing their true circular economy.

In this study, DP and AF are chosen as representative phosphorus FRs in PET due to their industrial importance, as well as different chemistry in controlling degradation reactions [27–30]. The flame retardancy and non-toxicity of both additives were already displayed by small-scale fire tests and preliminary toxicological evaluations, respectively [29,31,32]. DP is a novel FR additive that can be synthesized through green chemistry principles, and shows a promising lubrication action (i.e. decrease in the melt viscosity) during melt-processing of PET [27,33]. On the other hand, AF is a commercial phosphorus FR that can potentially compensate for PET degradation by reacting with the PET chains, leading to an increase in its melt viscosity [29]. Therefore, DP and AF can be good representatives to show the possible range of interactions occurring between phosphorus FRs and PET. Understanding this range of interactions systematically is the main purpose of the present study since it enables designing PET/FR products that can be optimally recycled by a thermomechanical approach. To assess the synergistic effects of these phosphorus FRs in PET, a systematic study was carried out, where the effects of these chemicals on major degradation pathways (i.e. thermal, thermo-oxidative, and thermomechanical) are evaluated by thermal and rheological investigations. A particular emphasis was put on the effects of those FRs on the mechanical behavior of the solid polymer [27,34,35]. Thus, we simulated a conventional thermomechanical recycling process by repeated melt extrusion and injection molding to examine how the incorporation of the additives alters the polymer behavior after recycling. Therefore, the recycling study performed here holds significant value in the development of phosphorus FRs for the sustainable processing of polyesters. This work aims at providing a starting point for the future synthesis of a series of multifunctional additives with similar phosphorus chemistry, which, in addition to their primary FR function, can answer to the increasing demands of sustainability and reprocessing of thermoplastic materials, leading to an improvement (or at least preserving) of PET stability and performance over extended life cycles.

2. Experimental details

2.1. Materials and processing

PET with an average molecular weight $M_w \approx 67{,}400$ g/mol and polydispersity index PDI = 2.47 was provided by Serge Ferrari Tersuisse AG (Emmenbrücke, Switzerland). DP was synthesized according to the procedure described in detail by Salmeia et al. [33], and AF was purchased from Thor GmbH (Germany). All materials were carefully dried before processing and/or testing at different stages to minimize hydrolytic degradation. PET was vacuum dried at 90 mbar in three steps: (i) 8 h at 100 °C, (ii) 2 h at 120 °C, and (iii) 4 h at 140 °C. The FRs were put in the vacuum oven at 90 mbar for two days at a temperature of 80 °C.

PET/FR compounds were prepared in the micro-compounder MC 15 HT (Xplore Instruments BV, The Netherlands). The micro-compounder is a small extrusion unit equipped with co-rotating screws that allows achieving a homogeneous melt compound thanks to its side recirculation channel. PET compounds containing either 5 wt.% of DP, or 3 wt.% of AF, were produced to obtain approximately similar phosphorus contents, see Table 1. This amount of phosphorus is known to yield FR properties with Limiting Oxygen Index (LOI) values above 26%, indicating a self-extinguishing behavior [28,36]. Moreover, pristine PET was processed under the same conditions as reference for comparison. Un-processed and processed PET are named uPET and pPET hereof, respectively.

Physically mixed PET and FR additives were fed (weighing a total of ~21 g to fill the micro-compounder capacity of 15 mL) into the micro-compounder at 285 °C (corresponding to a steady-state measured melt temperature of 277 °C), and mixed for 5 min at 50 rpm. The compounding conditions were carefully selected according to our previous studies to obtain homogeneous compounds, as well as to minimize thermo-mechanical polymer degradation at this stage [27–29]. The compounding was carried out under continuous nitrogen (N_2) flow (from the inlet into the micro-compounder) to avoid any thermo-oxidative degradation caused by air. After compounding, different blends were ground in a mechanical granulator (Hellweg, Germany) and hot-pressed at 300 °C with a hydraulic press (Lindenberg Technics AG, Switzerland) to produce 1 mm thick films for further analyzes.

2.2. Thermomechanical recycling trials

Thermomechanical recycling trials were carried out to assess the behavior of PET/FR compounds in repeated processing cycles, see Fig. 2. First, PET was compounded with DP or AF in a twin-screw extruder (ZK 16 mm × 36 L/D, Collin Lab & Pilot Solutions, Germany) equipped with a gravimetric side feeding system to obtain pellets with the desired FR concentration. Pure PET was also processed under similar conditions for sake of comparison. Afterward, the pellets were processed three times in a single-screw extruder (Rheomex OS 19 mm × 25 L/D, Germany) to reproduce multiple recycling conditions. Before each extrusion cycle, the pellets were dried in a vacuum oven for 4 h at 120 °C, followed by another 4 h at 140 °C. The achieved phosphorus contents after compounding and repeated extrusion cycles are summarized in Table 2. The temperature profiles of the twin-screw and single-screw extruders are given in Tables 3 and 4, respectively. A key advantage of processing PET/DP over pure PET and PET/AF is the profound lubrication effect of DP that allows for a substantial reduction of the pro-

Table 1
Sample formulations investigated in the rotational rheometer. uPET and pPET refer to the unprocessed and processed pure PET, respectively. Estimated and measured phosphorus contents (P-contents) of the samples are also given in the table. The measured P-contents are the average of five measurements by using the inductively coupled plasma optical emission spectrometry (ICP-OES) method.

Sample	Nominal FR content (wt.%)	Estimated P-content (wt.%)	Measured P-content (wt.%)
uPET	–	–	–
pPET	–	–	–
PET-5DP	5.0% DP	0.78	0.73 ± 0.02
PET-3AF	3.0% AF	0.72	0.68 ± 0.01

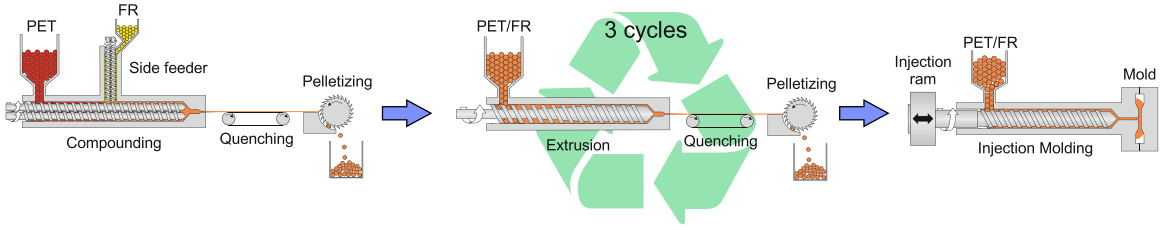

Fig. 2. Schematic representation of the thermomechanical recycling trials.

Table 2
List of samples investigated in the thermomechanical recycling trials. The prefixes "Co" and "*Re*" indicate the samples achieved after the compounding step in the twin-screw extruder, and after the recycling step in the single-screw extruder, respectively. P-content values from theory and measurements (five measurements per sample) are also given in the table.

Sample	Nominal FR content (wt.%)	Estimated P-content (wt.%)	Measured P-content (wt.%)
Co PET	–	–	–
Co PET-5DP	5.0% DP	0.78	0.70 ± 0.03
Co PET-3AF	3.0% AF	0.72	0.75 ± 0.01
Re PET	–	–	–
Re PET-5DP	5.0% DP	0.78	0.75 ± 0.01
Re PET-3AF	3.0% AF	0.72	0.69 ± 0.01

Table 3
Temperature profile of the twin-screw extruder in the compounding step.

Sample	Infeed (°C)	Pos. 1 (°C)	Pos. 2 (°C)	Pos. 3 (°C)	Pos. 4 (°C)	Pos. 5 (°C)	Pos. 6 (°C)	Nozzle (°C)
Co PET	70	300	305	305	305	305	305	290
Co PET-5DP	70	300	305	275	275	275	275	255
Co PET-3AF	70	295	295	295	295	295	295	275

Table 4
Temperature profile of the single-screw extruder in the recycling step.

Sample	Infeed (°C)	Pos. 1 (°C)	Pos. 2 (°C)	Pos. 3 (°C)	Pos. 4 (°C)	Pos. 5 (°C)	Nozzle (°C)
Re PET	15	295	295	295	295	295	307
Re PET-5DP	15	280	280	280	280	280	291
Re PET-3AF	15	295	300	300	300	300	310

cessing temperature. Benefiting from this merit, the extrusion temperatures used for processing PET/DP compounds were decreased by ~15 - 30 °C while the melt pressure was maintained.

After the extrusion cycles, the pellets were injection molded to obtain dog-bone specimens for investigating the mechanical properties by tensile tests. The process was carried out in an injection molding machine (Allrounder 320C Arburg, Germany) with the injection parameters summarized in Table 5.

Table 5
Processing parameters used in injection molding.

Barrel and mold temperatures (°C)		Injection pressures and times	
Infeed	60	Injection velocity (cm^3/s)	30
Barrel Pos. 1	265	Back pressure (bar)	50
Barrel Pos. 2	270	Injection pressure (bar)	1400
Barrel Pos. 3	275	Holding pressure (bar)	1300
Barrel Pos. 4	280	Holding pressure time (s)	11
Nozzle	285	Cooling time (s)	50
Mold	40	Total cycle time (s)	66.2

2.3. Characterization techniques

2.3.1. Rotational rheometer

Rheological measurements at low shear rates were carried out using a Physica 301 MCR rotational rheometer (Anton Paar, Austria) in a parallel plate geometry with a 25 mm diameter and a constant gap of 1 mm. The tests were conducted on samples cut out from hot-pressed films prepared as described before. The samples were dried in the vacuum oven before testing and were kept under an argon atmosphere during handling to avoid any possible moisture intake. In all of the experiments carried out in the rotational rheometer, the polymer plates were allowed to melt and

Table 6
Set temperatures of the metal casing and their corresponding measured values in the polymer melt.

Casing temperature (°C)	Melt temperature (°C)
265	257
275	266
285	277
295	288
305	297
315	307

equilibrate in the chamber for 120 s before starting the measurements.

Thermal and thermo-oxidative degradation pathways were examined under N_2 and air flow into the measuring chamber, respectively. Time-resolved frequency sweep (TRFS) runs were performed at three different temperatures of 265, 285, and 305 °C. Angular frequency was varied between 0.126 rad/s and 500 rad/s, with 5 points per decade. The applied strain was constant at 1% to maintain linear viscoelastic behavior. Each experiment probed the rheological response for ~2 h over 10 frequency sweep runs conducted on each sample. Before starting the test and between the frequency sweep runs, the sample was allowed to rest for 60 s to minimize its deformation history and temperature variations.

In addition to TRFS, constant shear rate (CSR) rotational tests were carried out at 0.1 s^{-1} for 90 min at 285 and 305 °C under N_2 and air atmospheres. With these experiments, one can compare the effects of low-intensity unidirectional shearing flows with small-amplitude oscillatory shearing flows. Samples were rested in the rheometer for 60 s before starting the measurement.

2.3.2. Micro-compounder

In addition to the mixing of PET/FR compounds, the micro-compounder MC 15 HT (Xplore Instruments, The Netherlands) was used for rheological characterization of the melt at high-intensity shearing flows over time. The compounds were processed inside the micro-compounder in recirculation for 1 h and the mixing torque was measured. Longer mixing times were avoided to prevent an excessive decrease of the melt viscosity, which could lead to lower precision in torque measurement as well as to possible leakage and damage of the screws. Pristine PET, PET-2DP (PET compound containing 2 wt.% DP), PET-5DP, and PET-3AF were tested at different set temperatures ranging between 265 °C and 315 °C depending on the compound. These temperatures represent the set values of the micro-compounder metal casing. The real temperature of the polymer melt was separately measured by a sensor directly in contact with the material, see Table 6. Once the feeding step was completed according to the description given before, the materials were mixed for 60 s at 285 °C and 50 rpm. Afterward, the temperature was changed to the desired set value and let stabilize for another 4 min. Torque was measured over time after these steps.

2.3.3. Gel permeation chromatography

Gel Permeation Chromatography (GPC) analyzes were carried out on samples obtained after 1 h of processing in the micro-compounder. Around 10–15 mg of material were dissolved in 5 mL of Hexafluoroisopropanol (HFIP) and then filtered with PTFE membrane filters (pore size of 0.45 μm) to remove large residuals that could invalidate the measurement. The solution was let pass through a Viscotek GPC max VE 2001 (Malvern Panalytical, UK) solvent/sample module equipped with a Viscotek TriSEC model 302 detector unit (Malvern Panalytical, UK). Measurements were performed with a Waters Styragel HT (4/10 μm particle size) column (Waters Corporation, MA, USA), after calibration with PMMA standards. The measurement conditions that were chosen are the following: column temperature of 23 °C, flow of 1 mL/min of HFIP as the solvent, and injection volume of 50 μL.

2.3.4. Elemental analysis

The phosphorus content was measured at different stages to assess the FR content in each sample. The analysis was performed with an Optima 3000 device (PerkinElmer AG, Switzerland) by using the inductively coupled plasma optical emission spectrometry method (ICP-OES). Around 200 mg of material were mixed in 3 mL of HNO_3 and then digested in the microwave. Each measurement was repeated five times on different spots of each sample.

2.3.5. Nuclear magnetic resonance spectroscopy

Nuclear magnetic resonance (NMR) spectroscopy was carried out to explore possible interactions between the two additives and the polymer during high-temperature heating cycles in the molten state. Around 100 mg of samples collected from rheological measurements and continuous reprocessing in the micro-compounder were dissolved in 700 μL of HFIP and analyzed. $^{31}P\{^1H\}$ NMR spectra were obtained at ambient temperature using a Bruker AV-III400 spectrometer (Bruker Biospin AG, Switzerland). ^{31}P chemical shifts were referenced to an external standard of neat H_3PO_4 (δ = 0.0 ppm).

2.3.6. Thermogravimetric analysis

Thermogravimetric analysis (TGA) of the compounds was performed with a TG209 F1 Iris apparatus (Netzsch, Germany). Approximately 5 mg of each sample were subjected to a heating ramp from 25 °C to the final desired temperature (285 °C or 305 °C) with a heating rate of 10 °C/min, which was then followed by an isothermal step for 3 h. The analyzes were done either in air or in N_2 with an overall gas flow of 50 mL/min.

2.3.7. Differential scanning calorimetry

Differential scanning calorimetry (DSC) was carried out with a DSC 14 Polyma instrument (Netzsch, Germany). For each measurement, around 10 mg of material were used. The samples were subjected to two heating runs from 25 to 300 °C, interspersed by a cooling step back to room temperature. The heating/cooling rate was set at 10 °C/min, and all experiments were performed under N_2 atmosphere (gas flow of 100 mL/min). The crystallinity degree (χ) was calculated considering an enthalpy of fusion (ΔH_f) of 140 J/g for the completely crystalline PET [37].

2.3.8. Tensile testing

Tensile tests were performed on a Zwick Z100 machine (Zwick-Roell AG, Germany) according to the standard ISO 527 to characterize the mechanical behavior of compounds. The results were obtained from an average of five tests for each blend. The analyzed dog-bone specimens (Type 1A shape) were conditioned for two weeks in a controlled environment at 23 °C and 50% relative humidity before testing. A load cell with a maximum capacity of 5 kN was used, and a testing speed of 50 mm/min was adopted for the experiments. True stress-strain curves were calculated from the experimental data similar to previous publications to account for the changes in the cross-section of samples during the tensile measurements [38–40].

3. Results and discussion

3.1. Thermal stability of PET/FR compounds

In thermomechanical recycling of PET/FR, the molten compounds must be stable at high (re)processing temperatures to preserve material properties. The influence of FR additives on PET stability at high temperatures is investigated by isothermal TGA

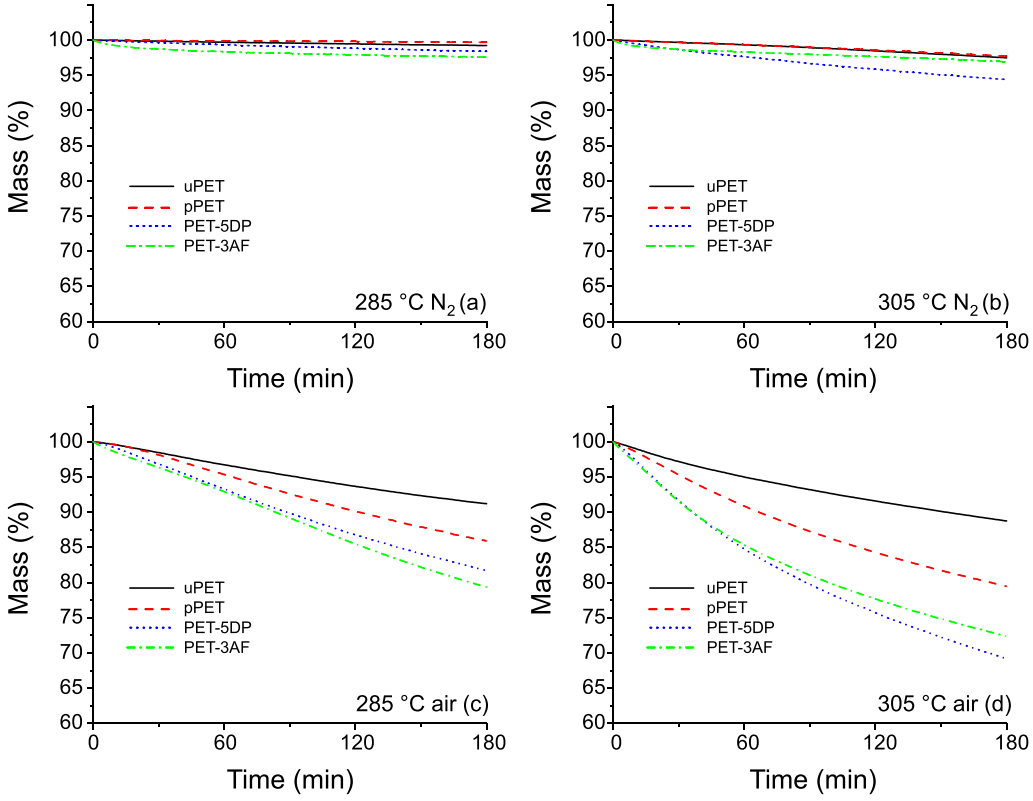

Fig. 3. Isothermal TGA graphs at different temperatures and atmospheres for the PET/FR samples: (a) 285 °C in N_2, (b) 305 °C in N_2, (c) 285 °C in air, (d) 305 °C in air.

experiments (Fig. 3). The PET/FR samples under examination are listed in Table 1. TGA results under N_2 show that the blends with FR additives do not exhibit any significant changes in thermal stability. They lose only ~1–3 wt.% of their mass after 3 h at both 285 °C and 305 °C. On the other hand, PET/ FR compounds show an early and increased mass loss compared to pPET under air atmosphere, indicating a stronger detrimental impact on PET stability. These results suggest that the thermo-oxidative degradation mechanisms are accelerated in PET by the phosphorus FRs under these experimental conditions. It is noteworthy that the thermal stability of PET/DP at lower temperatures (200 °C) in air is similar to (or even better than) that of pure PET [28]. A particular observation indicates that PET/AF degrades less than PET/DP at 305 °C (both in N_2 and air), even though pure AF has a lower thermal stability than pure DP (see Fig. 4). Therefore, one can assume that the thermal and thermo-oxidative degradation mechanisms of PET/AF change as the temperature is increased from 285 to 305 °C. In consequence, it is important to investigate the effects of the altered mechanisms on the stability of molten PET. In particular, once the mechanical stresses are introduced in the system during melt-processing, the temperature and/or oxygen effects could be either synergistic or antagonistic by the mechanical stresses [9].

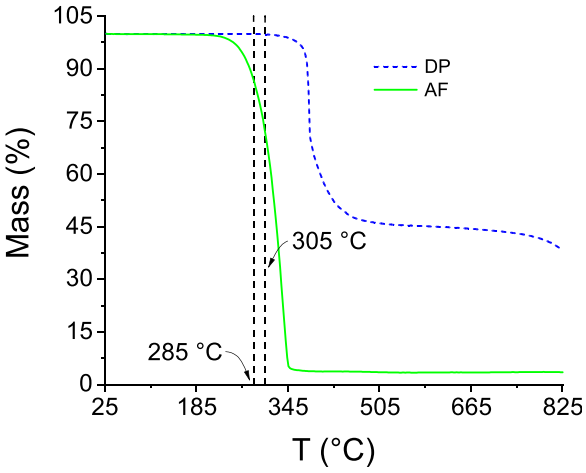

Fig. 4. TGA data of pure FR additives. Vertical dashed lines indicate the testing temperatures in Fig. 3 (285 °C and 305 °C).

3.2. Rheological behavior of PET/FR compounds

To carry out thermomechanical recycling of waste PET/FR, it is important to control the degradation mechanisms under mechanical stresses that are applied to the material during reprocessing. Hence, a detailed investigation of the rheological properties of molten PET by using the rotational rheometer is illuminating here.

In CSR experiments under air atmosphere (dashed black lines in Fig. 5), a slight initial reduction is observed in shear viscosities of uPET and pPET due to thermo-oxidative degradation [27,41,42]. Nevertheless, the viscosity reduction is slowed down after a certain time (~30 min at 305 °C and ~60 min at 285 °C), and the viscosity curves reach a plateau indicating an equilibrium between thermo-oxidative degradation and chain coupling (i.e. chain extension, branching, and/or crosslinking) [42]. In contrast, the PET-5DP sample displays a slow monotonic decline over the entire experimental window, with a deceleration of degradation towards the end. This observation suggests that either some degradation mechanisms are slightly fortified by DP, or the coupling reactions are hindered. Previous studies revealed that DP molecules can break down into radical species and initiate degradation attacks on PET chains [27].

The situation completely changes in PET-3AF with the compound showing a remarkable increase of viscosity over time due

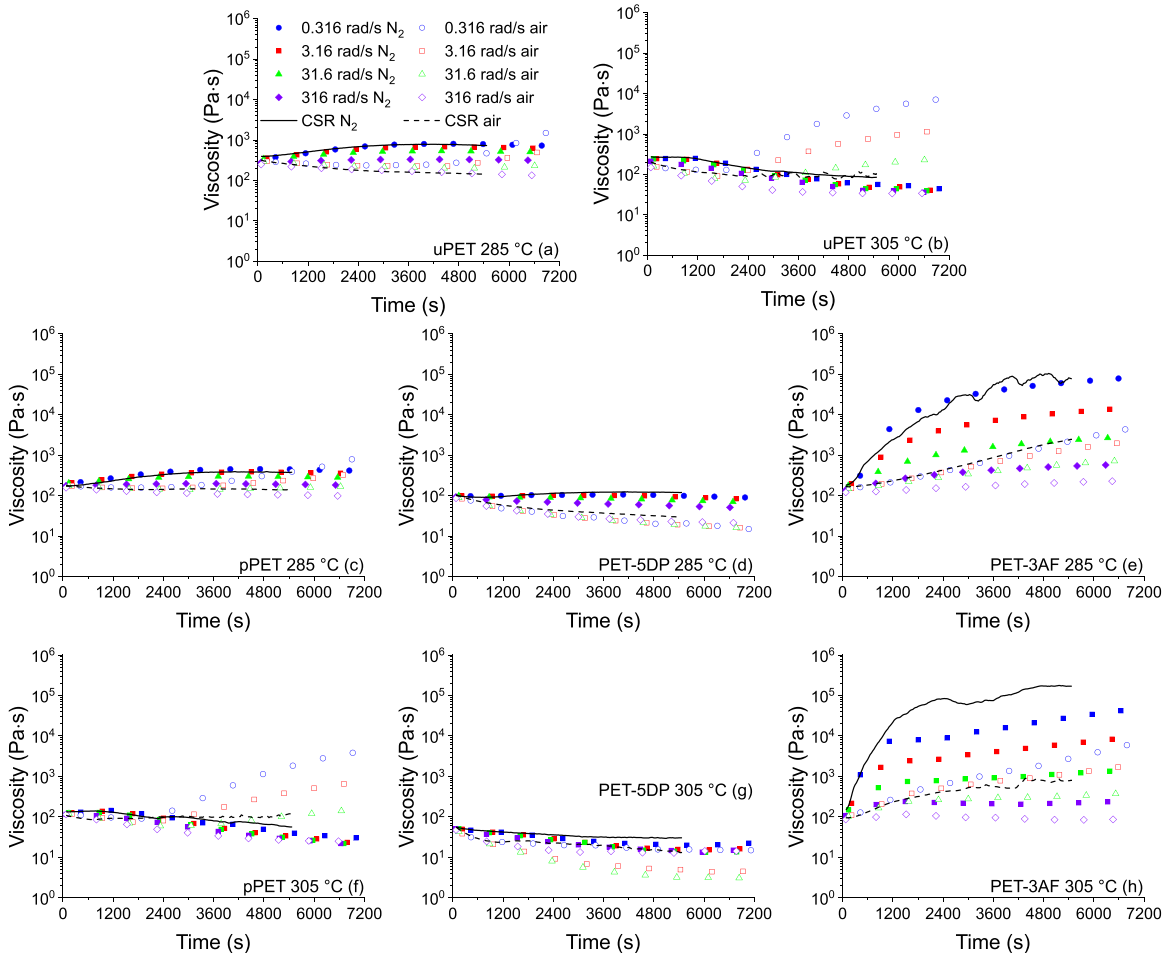

Fig. 5. Time-dependent behavior of complex viscosity for (a) uPET at 285 °C, (b) uPET at 305 °C, (c) pPET at 285 °C, (d) PET-5DP at 285 °C, (e) PET-3AF at 285 °C, (f) pPET at 305 °C, (g) PET-5DP at 305 °C, (h) PET-3AF at 305 °C. Full and empty markers represent different angular frequencies of TRFS experiments in N_2 and air, respectively, as shown in part a. The solid and dashed black lines show CSR shear viscosity experiments in N_2 and air, respectively, as shown in part a.

to the branching and/or crosslinking of chains [27,29,41]. It can be noticed that the branching kinetics in the first 30 min at 305 °C is faster than at 285 °C. However, the branching effect is saturated at longer times and balances with the decomposition mechanisms. A controlled branching reaction as the one portrayed in the compound with AF could be considered beneficial since it could help to maintain or enhance the melt viscosity of the polymer (theoretical higher M_w). Moreover, it can enable the application of such branched structures in certain processes, such as foaming or blow molding, which require a high melt strength to be performed [2,43,44].

Under N_2 environment, uPET, pPET, and PET-5DP (solid black lines in Fig. 5) are controlled by a competition between polycondensation and decomposition pathways as indicated by the constant shear viscosity [2,41,45]. On the other hand, PET-3AF compound illustrates a much steeper enhancement of melt viscosity over time in N_2 than in air. This significant difference suggests that polycondensation and branching reactions are hindered by the presence of oxygen.

For further analysis, the TRFS results are shown by markers in Fig. 5. The CSR curves are in good agreement with TRFS at low angular frequencies of 0.316 and 3.16 rad/s in almost all of the samples. However, the shear and complex viscosity data show different trends when uPET and pPET are analyzed under air at 285 °C (Fig. 5a,c). In these samples, an increase of viscosity can be observed mainly at low frequencies in TRFS due to oxidative branching/crosslinking reactions [41]. This behavior is strongly intensified at a higher temperature of 305 °C (Fig. 5b,f). In this case, the higher temperature eases overcoming the activation energy barrier and/or speeds up the branching kinetics [27,41]. In addition to a significant reduction in mechanical properties, the phenomenon of excessive oxidative branching/crosslinking can be highly detrimental for PET reprocessing, because it can cause a complete blockage of the extruder after a few cycles [42,46], severely limiting the recyclability of the polymer in some cases.

As opposed to pristine PET, the oxygen-induced increase of viscosity is absent in PET-5DP (Fig. 5d,g). Furthermore, DP shows a lubricating effect in the blend that allows for a reduction of the processing temperature [27]. It is important to control this lubrication (for instance, by lowering the temperature), since too low melt viscosity values can limit the pressure generation in industrial extrusion applications, such as melt-spinning of flame retardant fibers. By comparing the viscosity curves of pPET and PET-5DP at different temperatures under N_2 (Fig. 6a), it is evident that their viscosities are almost equal at testing temperatures of 285 °C and 265 °C, respectively. Moreover, the PET-5DP compound does not show any signs of branching in the air (Fig. 6b), in contrast to pPET, which is a further advantage for its thermomechanical recycling. Lower (re)processing temperatures can improve material stability by limiting thermal and thermo-oxidative degradation mechanisms, which can lead to improved thermomechanical recyclability of PET compounds. Together with flame retardancy, non-

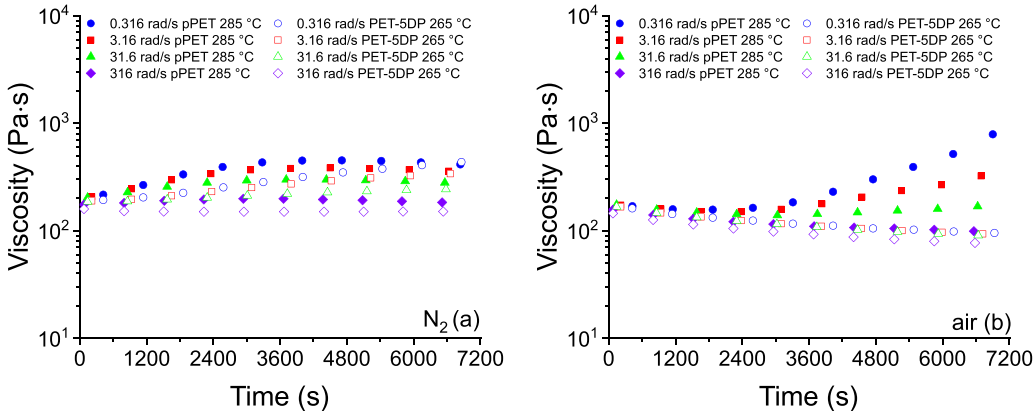

Fig. 6. Time-dependent behavior of complex viscosity for (a) pPET at 285 °C and PET-5DP at 265 °C both in N_2, (b) pPET at 285 °C and PET-5DP at 265 °C both in air. Markers with different colors represent different angular frequencies in TRFS experiments.

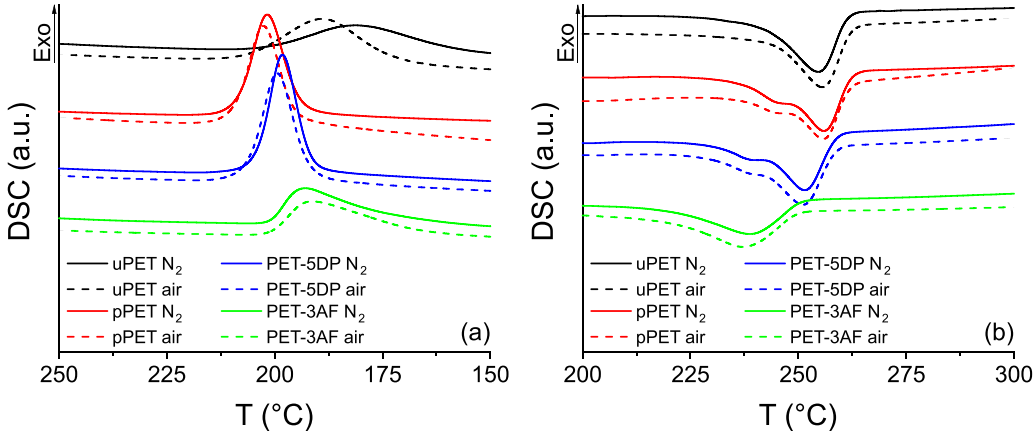

Fig. 7. DSC diagrams of (a) cooling and (b) second heating run, for the compounds *after* analysis by the rotational rheometer in TRFS at 285 °C.

Table 7
DSC data of the compounds *after* hot press and *before* analysis with the rotational rheometer.

Sample	T_m (°C)	T_c (°C)	χ (%)
uPET	254.1	182.0	21.3
pPET	255.3	199.8	23.5
PET-5DP	252.9	200.1	26.1
PET-3AF	250.4	196.5	22.8

toxicity, and the capability to hinder oxidative crosslinking, these properties make DP an attractive multifunctional additive for PET.

TRFS tests of PET-3AF show a similar gradual increase of viscosity over time (similar to CSR), which is more dominant under N_2. DSC data summarized in Tables 7 and 8 support the occurrence of branching/crosslinking reactions in the presence of AF. Branching typically leads to a decrease of crystallization degree (χ), lower crystallization and melting temperatures (T_c and T_m, respectively), accompanied by a broadening of the crystallization and melting peaks (Fig. 7) [37,47]. In particular, the PET-3AF sample (obtained *after* rheological analysis at 305 °C under N_2) displays a T_c shifted by ~30 °C compared to pPET and PET-3AF *before* analysis in the rheometer. In the case of uPET and pPET, a stronger chain scission results in a slightly better chain packing and crystallization, consequently with a small shift of T_c and T_m towards higher values. Furthermore, it is interesting to observe that the experiments at 265 °C under N_2 reveal a slight reduction of T_c and T_m, possibly due to the limited polycondensation occurring under these conditions. In contrast, the sample with DP does not follow the same trends. Despite the increasing degradation depicted by the complex viscosity curves, crystallization and melting peaks shift towards lower temperatures probably due to a better mixing between polymer and additive [27,28]. Further studies should be conducted to explain this behavior.

To further confirm the dominance of branching structures that occur during rheological trials, dissolution tests were performed in m-cresol at 120 °C. These experiments were carried out on sample residues *after* testing in the TRFS at 285 °C under N_2. In addition, the uPET sample that showed a significant increase in complex viscosity in air was also tested. The sample with DP (number 3 in Fig. 8), and both pure polymer samples (numbers 1 and 2 in Fig. 8), dissolved completely in m-cresol. In contrast, the branched samples PET-3AF and uPET tested in air (numbers 4 and 5 in Fig. 8, respectively), dissolved only partially. This observation further confirms the formation of highly branched structures during rheometry.

During thermomechanical recycling, the plastic experiences strong shearing stresses in repeated processing cycles. As such, it is important to characterize the melt stability of PET/FR compounds under high shearing intensities. Thus, complementary experiments were performed in the micro-compounder. The evolution of the mixing torque of the micro-compounder over time is shown in Fig. 9. It is clear that the melt behavior under strong shearing differs from the low-intensity flows in the rotational rheometer, showing a more pronounced decay over time. Pristine PET (uPET) and PET/DP compounds (PET-2DP and PET-5DP) exhibit a significant decrease in torque. In fact, the shear degradation introduced

Table 8
DSC data of the compounds *after* analysis with the rotational rheometer under different conditions.

TRFS temp.	265 °C			285 °C			305 °C		
Sample	T_m (°C)	T_c (°C)	χ (%)	T_m (°C)	T_c (°C)	χ (%)	T_m (°C)	T_c (°C)	χ (%)
under N_2									
uPET	253.7	177.3	21.7	254.7	181.5	25.2	256.0	199.4	29.3
pPET	255.0	199.3	27.1	255.9	201.7	26.5	256.7	203.4	25.8
PET-5DP	251.6	198.7	26.2	251.4	198.2	25.2	250.8	197.3	28.3
PET-3AF	244.9	192.6	17.9	238.7	193.0	19.5	242.3	167.3	20.2
under air									
uPET	254.3	188.3	26.4	255.5	189.0	25.1	255.6	199.3	27.4
pPET	255.6	202.6	27.6	255.9	202.6	21.5	255.7	203.6	25.6
PET-5DP	252.4	201.1	24.7	251.0	199.4	26.4	246.5	194.0	27.9
PET-3AF	245.2	194.2	21.0	237.2	191.0	19.8	244.0	183.3	22.5

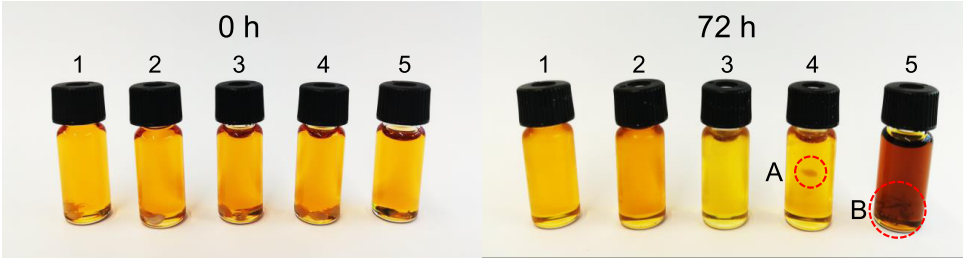

Fig. 8. Dissolution samples immediately after (left group), and 72 h after (right group) immersion in m-cresol at 120 °C. The samples were obtained *after* analysis by the rotational rheometer in TRFS experiments. The samples in each group from left to right are: (1) uPET at 285 °C in N_2, (2) pPET at 285 °C in N_2, (3) PET-5DP at 285 °C in N_2, (4) PET-3AF at 285 °C in N_2, (5) uPET at 305 °C in air. Red dashed circles A and B indicate residues in samples 4 and 5, respectively.

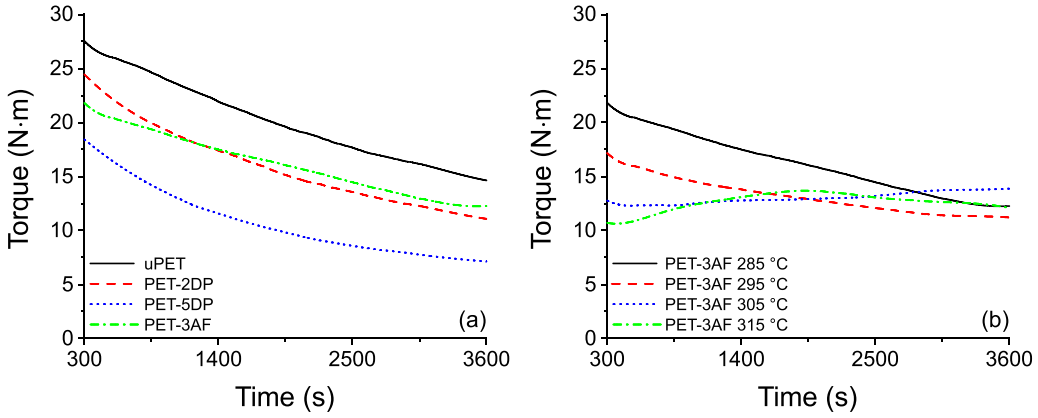

Fig. 9. Comparison of mixing torque of the micro-compounder for (a) uPET, PET-2DP, PET-5DP, and PET-3AF at 285 °C and 50 rpm, and (b) PET-3AF at 50 rpm under different temperatures.

by the micro-compounder strongly promotes polymer chain scission and becomes the main degradation mechanism [48]. In the PET-3AF sample (Fig. 9b), the steep branching observed before is overwhelmed by the strong shearing, particularly at lower processing temperatures (285 and 295 °C). Nevertheless, the branching mechanism becomes more pronounced at temperatures above 305 °C.

After these experiments, samples were taken from the micro-compounder and tested by DSC and GPC to verify the presence of branched structures. The shift of χ, T_m and T_c to lower values (see Table 9), the increase of M_w and PDI (see Table 10), together with the increase of torque over time, support significant PET branching reactions that occur at these temperatures in the presence of AF. It is noteworthy that thermal and thermo-mechanical degradation effects also become stronger at the highest testing temperature (315 °C), thus, competing more strongly with branching effects.

It is interesting to investigate the lubrication effect of DP on the recycling behavior of PET by lowering the (re)processing temperature. According to the rheological investigations, the temperature can be reduced between 10–20 °C for 2–5 wt.% of DP. One might expect that a decrease in the extrusion temperature could lead to a decrease in the overall degradation. However, the GPC results presented in Table 10 show that the PET-5DP sample processed at 265 °C has a lower M_w in comparison to the uPET sample processed at 285 °C (34.6 kg/mol and 39.8 kg/mol, respectively). Thus, the degradation mechanisms of PET-5DP are expected to be stronger than those of uPET under these testing conditions. Still, processing of PET-5DP at 265 °C, rather than at 285 °C, results in enhanced protection against thermal degradation as evidenced by its higher M_w value (34.6 kg/mol against 31.0 kg/mol).

Based on the presented results, previous studies on these FR additives [27,29], as well as complementary chemical analysis, degradation mechanisms of PET compounds containing DP or AF can be better understood, see the supplementary data.

Table 9
DSC data of samples *after* mixing for 1 h under different conditions in the micro-compounder.

uPET				PET-5DP				PET-3AF			
T (°C)/atm.	T_m (°C)	T_c (°C)	χ (%)	T (°C)/atm.	T_m (°C)	T_c (°C)	χ (%)	T (°C)/atm.	T_m (°C)	T_c (°C)	χ (%)
285/ N_2	255.2	203.5	24.4	265/ N_2	253.1	205.2	24.0	285/ N_2	249.4	197.5	27.6
295/ N_2	255.6	205.1	23.9	275/ N_2	252.8	205.1	24.4	295/ N_2	246.8	193.5	22.0
305/ N_2	255.9	203.7	25.8	285/ N_2	252.4	204.2	27.4	305/ N_2	243.9	191.5	20.8
285/ O_2	257.2	207.0	23.8	285/ O_2	253.0	206.4	25.6	315/ N_2	239.7	197.2	19.9

Table 10
Average molecular weight (M_w) and polydispersity index (PDI) values obtained from GPC measurements of uPET and other compounds *after* mixing at 50 rpm for 1 h in the micro-compounder.

Sample	Processing parameters		GPC results	
	T (°C)	Atmosphere	M_w (kg/mol)	PDI
uPET	not processed		67.4	2.47
uPET	285	N_2	39.8	2.17
PET-5DP	285	N_2	31.0	2.35
PET-5DP	265	N_2	34.6	2.14
PET-3AF	285	N_2	44.4	2.43
PET-3AF	305	N_2	118.0	6.44

Table 11
Summary of the mechanical properties obtained from tensile experiments: Young's modulus (E_t), maximum tensile stress (σ_m), tensile strain at maximum stress (ε_m), tensile strain at break (ε_b). In the case of the brittle *Re* PET-3AF, ε_m and ε_b are identical.

Sample	E_t (MPa)	σ_m (MPa)	ε_m (%)	ε_b (%)
uPET	2753 ± 42	69.5 ± 0.6	3.78 ± 0.02	15.73 ± 2.13
Co PET	2733 ± 52	68.7 ± 1.9	3.75 ± 0.08	21.34 ± 2.30
Co PET-5DP	2843 ± 67	72.5 ± 1.5	3.69 ± 0.05	12.45 ± 0.91
Co PET-3AF	2859 ± 66	71.8 ± 1.5	3.53 ± 0.07	10.52 ± 0.70
Re PET	2833 ± 14	69.8 ± 0.8	3.69 ± 0.04	17.65 ± 3.91
Re PET-5DP	2824 ± 63	71.1 ± 1.1	3.60 ± 0.02	12.12 ± 1.79
Re PET-3AF	2888 ± 18	70.4 ± 2.0	3.18 ± 0.19	3.18 ± 0.19

3.3. Thermomechanical recycling of PET/FR compounds

In the previous sections, we investigated the influence of DP and AF on the molecular stability of PET in the molten state, where they demonstrated different behavior in PET including enhanced lubrication and decreased chain scissions. It is important to assess their influence on the mechanical performance of recycled plastic waste to take advantage of the observed beneficial potentials in thermomechanical recycling. A satisfactory mechanical performance allows for re-using the recycled plastic in a closed-loop circular economy, and/or for upcycling of the recycled plastic by adding more pristine FRs. Therefore, mechanical characterization of PET/FR compounds was carried out by tensile experiments before and after thermomechanical recycling.

Tensile results of the samples obtained after an initial compounding step in the twin-screw extruder (see Fig. 2 for processing steps) are shown in Fig. 10a. It is clear that the incorporation of FRs in PET does not lead to material embrittlement. The PET/DP sample shows slightly higher elastic modulus and yield strength with a reduction in elongation at break (Table 11). On the other hand, PET/AF displays a substantial decrease in elongation at yield and elongation at break, considerably worsening ductility and toughness properties of the recycled plastic (Fig. 10a).

After the compounds undergo thermomechanical recycling, significant differences emerge between the compounds with or without phosphorus FRs (Fig. 10b). Pure PET, which has an average elongation at break of around ~21% after the compounding step, experiences a slight decrease of ~4% for this value. Moreover, its other mechanical properties remain almost unchanged after recycling. The small reduction in performance can be explained by thermo-mechanical degradation mechanisms during the repeated processing steps, leading to a decline in polymer molecular weight [49]. It is noteworthy that the PET sample containing DP exhibits a similar mechanical behavior compared to its counterpart after compounding. In fact, the performance of the compound is hardly influenced by the repeated processing. This observation suggests that PET/DP compounds are highly stable materials, both from rheological and mechanical perspectives, and that they can be recy-

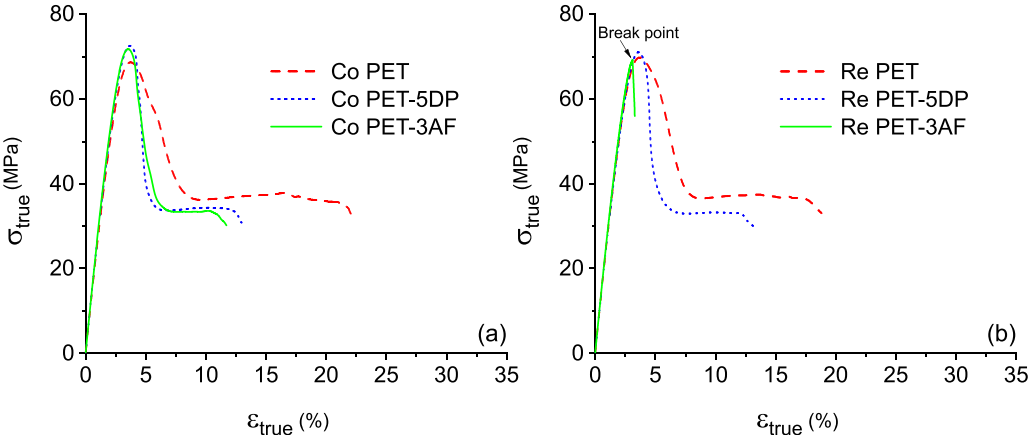

Fig. 10. True stress-strain curves for PET compound: (a) Co PET, Co PET-5DP and Co PET-3AF, (b) *Re* PET, *Re* PET-5DP and *Re* PET-3AF. The breakpoint of the brittle *Re* PET-3AF sample is shown by an arrow in part b.

cled multiple times by a thermomechanical approach. Previous results have also shown that DP does not have any adverse effects on the mechanical flexibility of PET after high-temperature annealing [28]. In contrast, the recycled PET/AF compound undergoes a dramatic change in its tensile behavior after thermomechanical recycling, showing considerable embrittlement of all specimens investigated (Fig. 10b). This loss of toughness and ductility during recycling is ascribed to the excessive branching reactions that can lead to a drastic change of M_w and PDI (see Table 10) [50]. Therefore, thermomechanical recycling of PET/AF waste can hardly lead to high-quality material streams for circular production.

4. Conclusion

Degradation mechanisms during thermomechanical recycling of PET/FR compounds were investigated for two eco-friendly phosphorus FRs, namely DP and AF. Here, we mainly focused on (i) thermal, (ii) thermo-oxidative, and (iii) thermo-mechanical degradation pathways by utilizing different experimental techniques including thermal, rheological, chemical, and mechanical analysis. Pristine PET showed oxidative branching/crosslinking in rheological tests under low-intensity shearing flows. This detrimental phenomenon was completely hindered by the addition of DP, which is a significant advantage for the recycling of PET. Moreover, PET/DP compounds showed a substantial lubrication effect, allowing for a reduction of the processing temperature (~20 °C for 5 wt.% of DP), which reduces the thermal decomposition of PET during its extrusion. In contrast, PET/AF compounds displayed a significant increase in viscosity over time, which is ascribed to accelerated branching reactions. Based on DSC results, this behavior is more pronounced under inert N_2 atmosphere and at higher temperatures. The formation of highly crosslinked structures in the PET melt was also confirmed by dissolution tests. Moreover, micro-compounding trials elucidated thermo-mechanical degradation of PET/FR compounds under strong shearing flows, as they occur in repeated reprocessing cycles. In these experiments, PET/DP compounds showed no advantage in controlling the degradation mechanisms in comparison to pristine PET. PET/AF compounds, on the other hand, demonstrated branching reactions that depend on the processing temperature. This branching led to a broadening of the molecular weight distribution of PET as shown by GPC experiments, as well as to a downward shift of crystallization and melting temperatures as shown by DSC experiments. Based on these results, supported by NMR spectroscopy and phosphorus content measurements, chemical reaction mechanisms were proposed for the degradation of PET/FR compounds. It was concluded that both additives partially decompose at elevated temperatures, leading to the formation of phosphorus radicals that trigger the degradation and branching reactions in DP and AF, respectively. Additionally, a thermomechanical recycling process was created, in which the PET/FR compounds were processed by multiple extrusion and injection molding cycles. This allowed investigating the mechanical properties of the compounds by tensile experiments before and after recycling. The respective results show that the branching reaction in PET/AF leads to a significant downgrading of its mechanical performance after repeated recycling, and that the recycled plastic shows a brittle behavior. On the other hand, DP-containing PET maintained its ductile mechanical performance after recycling, similar to pristine PET. These observations are extremely encouraging for designing PET/FR products for recycling through a thermomechanical approach benefitting from novel eco-friendly phosphorus chemistry.

Declaration of Competing Interest

The authors declare that they have no known competing financial interests or personal relationships that could have appeared to influence the work reported in this paper.

CRediT authorship contribution statement

Christopher Bascucci: Methodology, Investigation, Formal analysis, Writing – original draft, Writing – review & editing, Visualization. **Ivica Duretek:** Investigation, Formal analysis. **Sandro Lehner:** Investigation, Formal analysis. **Clemens Holzer:** Methodology, Writing – review & editing. **Sabyasachi Gaan:** Conceptualization, Methodology, Writing – review & editing. **Rudolf Hufenus:** Conceptualization, Methodology, Writing – review & editing. **Ali Gooneie:** Project administration, Conceptualization, Methodology, Formal analysis, Investigation, Writing – original draft, Writing – review & editing, Visualization.

Acknowledgments

For the funding of this research, the authors acknowledge the Zürcher Stiftung für Textilforschung (Switzerland), and Empa-Internal Research Call 2020 in the framework of the "RePET" project. The NMR hardware used for measurements in this work was partially granted by SNSF (Grant No. 150638). Serge Ferrari Tersuisse AG is thanked for providing PET. We also thank M. Lienhard and M. Hilber (both Empa) for their valuable assistance in performing experiments.

Supplementary materials

Supplementary material associated with this article can be found, in the online version, at doi:10.1016/j.polymdegradstab.2021.109783.

References

[1] S. Venkatachalam, G. Shilpa, V. Jayprakash, R. Prashant, K. Rao, K. Anil, Degradation and recyclability of poly (ethylene terephthalate), Polyester, InTech, 2012, doi:10.5772/48612.

[2] F. Awaja, D. Pavel, Recycling of PET, Eur. Polym. J. 41 (2005) 1453–1477, doi:10.1016/j.eurpolymj.2005.02.005.

[3] B. Geueke, K. Groh, J. Muncke, Food packaging in the circular economy: overview of chemical safety aspects for commonly used materials, J. Clean. Prod. 193 (2018) 491–505, doi:10.1016/j.jclepro.2018.05.005.

[4] R. Hufenus, Y. Yan, M. Dauner, T. Kikutani, Melt-spun fibers for textile applications, Materials 13 (2020) 4298 (Basel), doi:10.3390/ma13194298.

[5] L. Delva, S. Hubo, L. Cardon, K. Ragaert, On the role of flame retardants in mechanical recycling of solid plastic waste, Waste Manag. 82 (2018) 198–206, doi:10.1016/j.wasman.2018.10.030.

[6] Y. Pan, L. Liu, L. Song, Y. Hu, W. Wang, H. Zhao, Durable flame retardant treatment of polyethylene terephthalate (PET) fabric with cross-linked layer-by-layer assembled coating, Polym. Degrad. Stab. 165 (2019) 145–152, doi:10.1016/j.polymdegradstab.2019.05.009.

[7] P. Li, B. Wang, Y.J. Xu, Z. Jiang, C. Dong, Y. Liu, P. Zhu, Ecofriendly flame-retardant cotton fabrics: preparation, flame retardancy, thermal degradation properties, and mechanism, ACS Sustain. Chem. Eng. 7 (2019) 19246–19256, doi:10.1021/acssuschemeng.9b05523.

[8] S. Chang, X. Zhou, Z. Xing, T. Tu, Probing polarity of flame retardants and correlating with interaction between flame retardants and PET fiber, J. Colloid Interface Sci. 498 (2017) 343–350, doi:10.1016/j.jcis.2017.03.047.

[9] K. Ragaert, L. Delva, K. Van Geem, Mechanical and chemical recycling of solid plastic waste, Waste Manag. 69 (2017) 24–58, doi:10.1016/j.wasman.2017.07.044.

[10] G. Sandin, G.M. Peters, Environmental impact of textile reuse and recycling – a review, J. Clean. Prod. 184 (2018) 353–365, doi:10.1016/j.jclepro.2018.02.266.

[11] X. Wang, W. Wang, S. Wang, Y. Yang, H. Li, J. Sun, X. Gu, S. Zhang, Self-intumescent polyelectrolyte for flame retardant poly (lactic acid) nonwovens, J. Clean. Prod. 282 (2021) 124497, doi:10.1016/j.jclepro.2020.124497.

[12] R. Nayak, S. Houshyar, A. Patnaik, L.T. Nguyen, R.A. Shanks, R. Padhye, M. Fegusson, Sustainable reuse of fashion waste as flame-retardant mattress filing with ecofriendly chemicals, J. Clean. Prod. 251 (2020) 119620, doi:10.1016/j.jclepro.2019.119620.

[13] O. Horodytska, F.J. Valdés, A. Fullana, Plastic flexible films waste management – a state of art review, Waste Manag. 77 (2018) 413–425, doi:10.1016/j.wasman.2018.04.023.

[14] E. Van Eygen, D. Laner, J. Fellner, Circular economy of plastic packaging: current practice and perspectives in Austria, Waste Manag. 72 (2018) 55–64, doi:10.1016/j.wasman.2017.11.040.

[15] K. Pivnenko, K. Granby, E. Eriksson, T.F. Astrup, Recycling of plastic waste: screening for brominated flame retardants (BFRs), Waste Manag. 69 (2017) 101–109, doi:10.1016/j.wasman.2017.08.038.

[16] A. Castellano, C. Colleoni, G. Iacono, A. Mezzi, M.R. Plutino, G. Malucelli, G. Rosace, Synthesis and characterization of a phosphorous/nitrogen based sol-gel coating as a novel halogen- and formaldehyde-free flame retardant finishing for cotton fabric, Polym. Degrad. Stab. 162 (2019) 148–159, doi:10.1016/j.polymdegradstab.2019.02.006.

[17] P. Simonetti, R. Nazir, A. Gooneie, S. Lehner, M. Jovic, K.A. Salmeia, R. Hufenus, A. Rippl, J.P. Kaiser, C. Hirsch, B. Rubi, S. Gaan, Michael addition in reactive extrusion: a facile sustainable route to developing phosphorus based flame retardant materials, Compos. Part B Eng. 178 (2019) 107470, doi:10.1016/j.compositesb.2019.107470.

[18] S. Yasin, N. Behary, A. Perwuelz, J. Guan, Life cycle assessment of flame retardant cotton textiles with optimized end-of-life phase, J. Clean. Prod. 172 (2018) 1080–1088, doi:10.1016/j.jclepro.2017.10.198.

[19] F. Portet-Koltalo, N. Guibert, C. Morin, F. de Mengin-Fondragon, A. Frouard, Evaluation of polybrominated diphenyl ether (PBDE) flame retardants from various materials in professional seating furnishing wastes from French flows, Waste Manag. 131 (2021) 108–116, doi:10.1016/j.wasman.2021.05.038.

[20] F. Ronkay, B. Molnár, F. Szalay, D. Nagy, B. Bodzay, I.E. Sajó, K. Bocz, Development of flame-retarded nanocomposites from recycled PET bottles for the electronics industry, Polymers 11 (2019) 233 (Basel), doi:10.3390/polym11020233.

[21] S. Altun, Y. Ulcay, Improvement of waste recycling in PET fiber production, J. Polym. Environ. 12 (2004) 231–237, doi:10.1007/s10924-004-8150-4.

[22] M. Khoonkari, A.H. Haghighi, Y. Sefidbakht, K. Shekoohi, A. Ghaderian, Chemical recycling of PET wastes with different catalysts, Int. J. Polym. Sci. 2015 (2015) 1–11, doi:10.1155/2015/124524.

[23] C. Jehanno, I. Flores, A.P. Dove, A.J. Müller, F. Ruipérez, H. Sardon, Organocatalysed depolymerisation of PET in a fully sustainable cycle using thermally stable protic ionic salt, Green Chem. 20 (2018) 1205–1212, doi:10.1039/C7GC03396F.

[24] L.Nguyet Thi Ho, D.Minh Ngo, J. Cho, H.M. Jung, Enhanced catalytic glycolysis conditions for chemical recycling of glycol-modified poly(ethylene terephthalate), Polym. Degrad. Stab. 155 (2018) 15–21, doi:10.1016/j.polymdegradstab.2018.07.003.

[25] Plastics Europe, 2020. Plastics - the Facts 2020: An analysis of European plastics production, demand and waste data, Plastics Europe Brussels, Belgium. https://plasticseurope.org/.

[26] S.H. Park, S.H. Kim, Poly (ethylene terephthalate) recycling for high value added textiles, Fash. Text. 1 (2014) 1, doi:10.1186/s40691-014-0001-x.

[27] A. Gooneie, P. Simonetti, K.A. Salmeia, S. Gaan, R. Hufenus, M.P. Heuberger, Enhanced PET processing with organophosphorus additive: flame retardant products with added-value for recycling, Polym. Degrad. Stab. 160 (2019) 218–228, doi:10.1016/j.polymdegradstab.2018.12.028.

[28] A. Gooneie, P. Simonetti, P. Rupper, R. Nazir, M. Jovic, S. Gaan, M.P. Heuberger, R. Hufenus, Stabilizing effects of novel phosphorus flame retardant on PET for high-temperature applications, Mater. Lett. 276 (2020) 128225, doi:10.1016/j.matlet.2020.128225.

[29] K.A. Salmeia, A. Gooneie, P. Simonetti, R. Nazir, J.P. Kaiser, A. Rippl, C. Hirsch, S. Lehner, P. Rupper, R. Hufenus, S. Gaan, Comprehensive study on flame retardant polyesters from phosphorus additives, Polym. Degrad. Stab. 155 (2018) 22–34, doi:10.1016/j.polymdegradstab.2018.07.006.

[30] K. Salmeia, S. Gaan, G. Malucelli, Recent advances for flame retardancy of textiles based on phosphorus chemistry, Polymers 8 (2016) 319 (Basel), doi:10.3390/polym8090319.

[31] D. Goedderz, L. Weber, D. Markert, A. Schießer, C. Fasel, R. Riedel, V. Altstädt, C. Bethke, O. Fuhr, F. Puchtler, J. Breu, M. Döring, Flame retardant polyester by combination of organophosphorus compounds and an NOR radical forming agent, J. Appl. Polym. Sci. 137 (2020) 47876, doi:10.1002/app.47876.

[32] P. Samani, Y. van der Meer, Life cycle assessment (LCA) studies on flame retardants: a systematic review, J. Clean. Prod. 274 (2020) 123259, doi:10.1016/j.jclepro.2020.123259.

[33] K.A. Salmeia, G. Baumgartner, M. Jovic, A. Gössi, W. Riedl, T. Zich, S. Gaan, Industrial upscaling of DOPO-based phosphonamidates and phosphonates derivatives using Cl_2 gas as a chlorinating agent, Org. Process Res. Dev. 22 (2018) 1570–1577, doi:10.1021/acs.oprd.8b00295.

[34] M.M. Velencoso, A. Battig, J.C. Markwart, B. Schartel, F.R. Wurm, Molecular firefighting-how modern phosphorus chemistry can help solve the challenge of flame retardancy, Angew. Chemie Int. Ed. 57 (2018) 10450–10467, doi:10.1002/anie.201711735.

[35] C.A. Wilkie, A.B. Morgan, Fire Retardancy of Polymeric Materials, 2nd ed., CRC press, Boca Raton, USA, 2010.

[36] R. Nazir, A. Gooneie, S. Lehner, M. Jovic, P. Rupper, N. Ott, R. Hufenus, S. Gaan, Alkyl sulfone bridged phosphorus flame-retardants for polypropylene, Mater. Des. 200 (2021) 109459, doi:10.1016/j.matdes.2021.109459.

[37] J. Li, S. Tang, Z. Wu, A. Zheng, Y. Guan, D. Wei, Branching and cross-linking of poly(ethylene terephthalate) and its foaming properties, Polym. Sci. Ser. B. 59 (2017) 164–172, doi:10.1134/S1560090417020051.

[38] E. Perret, F.A. Reifler, A. Gooneie, K. Chen, F. Selli, R. Hufenus, Structural response of melt-spun poly(3-hydroxybutyrate) fibers to stress and temperature, Polymer 197 (2020) 122503 (Guildf), doi:10.1016/j.polymer.2020.122503.

[39] E. Perret, F.A. Reifler, A. Gooneie, R. Hufenus, Tensile study of melt-spun poly(3-hydroxybutyrate) P3HB fibers: reversible transformation of a highly oriented phase, Polymer 180 (2019) 121668 (Guildf), doi:10.1016/j.polymer.2019.121668.

[40] E. Perret, F.A. Reifler, A. Gooneie, K. Chen, F. Selli, R. Hufenus, X-ray data about the structural response of melt-spun poly(3-hydroxybutyrate) fibers to stress and temperature, Data Brief. 31 (2020) 105675, doi:10.1016/j.dib.2020.105675.

[41] M. Kruse, M.H. Wagner, Time-resolved rheometry of poly(ethylene terephthalate) during thermal and thermo-oxidative degradation, Rheol. Acta 55 (2016) 789–800, doi:10.1007/s00397-016-0955-2.

[42] L.K. Nait-Ali, X. Colin, A. Bergeret, Kinetic analysis and modeling of PET macromolecular changes during its mechanical recycling by extrusion, Polym. Degrad. Stab. 96 (2011) 236–246, doi:10.1016/j.polymdegradstab.2010.11.004.

[43] F. Daver, R. Gupta, E. Kosior, Rheological characterisation of recycled poly(ethylene terephthalate) modified by reactive extrusion, J. Mater. Process. Technol. 204 (2008) 397–402, doi:10.1016/j.jmatprotec.2007.11.090.

[44] P. Raffa, M.B. Coltelli, S. Savi, S. Bianchi, V. Castelvetro, Chain extension and branching of poly(ethylene terephthalate) (PET) with di- and multifunctional epoxy or isocyanate additives: an experimental and modeling study, React. Funct. Polym. 72 (2012) 50–60, doi:10.1016/j.reactfunctpolym.2011.10.007.

[45] M. Kruse, V.H. Rolón-Garrido, M.H. Wagner, Rheological characterization of degradation and polycondensation of poly(ethylene terephthalate) melt in air and in nitrogen, in: AIP Conference Proceedings, 2013, pp. 216–229, doi:10.1063/1.4802616.

[46] R. Assadi, X. Colin, J. Verdu, Irreversible structural changes during PET recycling by extrusion, Polymer 45 (2004) 4403–4412 (Guildf), doi:10.1016/j.polymer.2004.04.029.

[47] P. Kiliaris, C.D. Papaspyrides, R. Pfaendner, Reactive-extrusion route for the closed-loop recycling of poly(ethylene terephthalate), J. Appl. Polym. Sci. 104 (2007) 1671–1678, doi:10.1002/app.25795.

[48] Kruse, M. From Linear to Long-Chain Branched Poly(Ethylene Terephthalate) – Reactive Extrusion, Rheology and Molecular Characterization; Universitätsverlag der TU Berlin, 2017. http://dx.doi.org/10.14279/depositonce-5683.

[49] M. Frounchi, Studies on degradation of PET in mechanical recycling, Macromol. Symp. 144 (1999) 465–469, doi:10.1002/masy.19991440142.

[50] H. Arayesh, N. Golshan Ebrahimi, B. Khaledi, M.Khabazian Esfahani, Introducing four different branch structures in PET by reactive processing––a rheological investigation, J. Appl. Polym. Sci. 137 (2020) 1–11, doi:10.1002/app.49243.